J|A|C|S ARTICLES

Published on Web 07/06/2009

2D−3D Transition for Cationic and Anionic Gold Clusters: A Kinetic Energy Density Functional Study

Lara Ferrighi, Bjørk Hammer, and Georg K. H. Madsen*

Interdisciplinary Nanoscience Center (iNANO) and Department of Physics and Astronomy, Aarhus University, DK-8000 Aarhus C, Denmark

Received April 23, 2009; E-mail: georg.madsen@inano.dk

Abstract: We present a density functional theory study of the energetics of isolated Au_n^+ ($n = 5-10$) and Au_n^- ($n = 8-13$) gold clusters. We compare our results to both theoretical and experimental values from the literature and find the use of meta-generalized gradient approximation (MGGA) functionals, in particular the M06-L functional, to be of importance in order to match experiment. The M06-L values suggest crossovers between 2D and 3D structures at $n = 8$ and 12 for cationic and anionic clusters, respectively. We suggest that the MGGA's stronger tendency toward 3D structures arises from their smaller gradient enhancement. Moreover, we show how MGGAs, in contrast to generalize gradient approximations with smaller gradient enhancements, avoid overestimating the bond energies by combining the information contained in the reduced gradient and the kinetic energy. This allows MGGAs to treat differently the exchange enhancement in the decaying density and bonding regions.

Introduction

The fundamental interest in the structure and reactivity of gold nanoparticles has grown strongly after the discovery of their catalytic activity when dispersed on oxide supports.[1−3] Detailed reviews presenting different results achieved on the subject have been published.[4−7] One of the tools most frequently employed for understanding the reactivity of gold clusters has been the use of calculations based on the generalized gradient approximation (GGA) to density functional theory (DFT).[8−16] The GGAs are highly popular because of their computational simplicity, but some issues are still open with respect to their validity in this endeavor. In one recent example, it was shown how changing between two widely used GGA functionals changed the stable structures of adsorbed gold clusters.[17] When discussing the factors influencing the catalytic activity of gold clusters, different authors have focused on the charge state, the interaction with the support, and the shape and size of the particles.[8,13,18−24] All of these factors are interrelated, and with catalytic activity having been measured on clusters containing as few as 7−10 gold atoms,[25−28] the structure of small gold clusters is obviously an important issue.

In this respect, it is interesting that prediction of the cluster size at which a transition between two-dimensional (2D) and three-dimensional (3D) structures appears, both in Au_n^- and in Au_n^+ gas-phase clusters, has posed a long-standing challenge for DFT.[29] Ion mobility measurements,[30] photoelectron experiments,[31] and electron diffraction data[32] consistently show that anionic gold clusters assume a planar structure for $n \leq 11$,

(1) Haruta, M.; Yamada, N.; Kobayashi, T.; Iijima, S. *J. Catal.* **1989**, *115*, 301.
(2) Hayashi, T.; Tanaka, K.; Haruta, M. *J. Catal.* **1998**, *178*, 566.
(3) Bocuzzi, F.; Chiorino, A.; Manzoli, M.; Andreeva, D.; Tabakova, T. *J. Catal.* **1999**, *188*, 176.
(4) Haruta, M. *Gold Bull.* **2004**, *37*, 27.
(5) Meyer, R.; Lemire, C.; Shaikhutdinov, S. K.; Freund, H.-J. *Gold Bull.* **2004**, *37*, 72.
(6) Thompson, D. T. *Top. Catal.* **2006**, *38*, 231.
(7) Chen, M.; Goodman, D. W. *Chem. Soc. Rev.* **2008**, *37*, 1860.
(8) Molina, L. M.; Rasmussen, M. D.; Hammer, B. *J. Chem. Phys.* **2004**, *120*, 7673.
(9) Yoon, B.; Häkkinen, H.; Landman, U.; Wörz, A. S.; Antonietti, J. M.; Abbet, S.; Judai, K.; Heiz, U. *Science* **2005**, *307*, 403.
(10) Tong, X.; Benz, L.; Kemper, P.; Metiu, H.; Bowers, M. T.; Buratto, S. K. *J. Am. Chem. Soc.* **2005**, *127*, 13516.
(11) Hernández, N. C.; Sanz, J. F.; Rodriguez, J. A. *J. Am. Chem. Soc.* **2006**, *128*, 15600.
(12) Chrétien, S.; Metiu, H. *J. Chem. Phys.* **2008**, *128*, 044714.
(13) Mavrikakis, M.; Stoltze, P.; Nørskov, J. K. *Catal. Lett.* **2000**, *64*, 101.
(14) Matthey, D.; Wang, J. G.; Wendt, S.; Matthiesen, J.; Schaub, R.; Lægsgaard, E.; Hammer, B.; Besenbacher, F. *Science* **2007**, *315*, 1692.
(15) Coquet, R.; Howard, K. L.; Willock, D. J. *Chem. Soc. Rev.* **2008**, *37*, 1860.
(16) Landman, U.; Yoon, B.; Zhang, C.; Heiz, U.; Arenz, M. *J. Am. Chem. Soc.* **2007**, *129*, 2229.
(17) Madsen, G. K. H.; Hammer, B. *J. Chem. Phys.* **2009**, *130*, 044704.
(18) Bamwenda, G. R.; Tsubota, S.; Nakamura, T.; Haruta, M. *Catal. Lett.* **1997**, *44*, 83.
(19) Valden, M.; Lai, X.; Goodman, D. W. *Science* **1998**, *281*, 1647.
(20) Diemant, T.; Hartmann, H.; Bansmann, J.; Behm, R. J. *J. Catal.* **2007**, *252*, 171.
(21) Chen, M. S.; Cai, Y.; Yan, Z.; Goodman, D. W. *J. Am. Chem. Soc.* **2006**, *128*, 6341.
(22) Cosandey, F.; Madey, T. E. *Surf. Rev. Lett.* **2001**, *8*, 73.
(23) Fu, Q.; Saltsburg, H.; Flytzani-Stephanopoulos, M. *Science* **2003**, *301*, 935.
(24) Overbury, S.; Ortiz-Soto, L.; Zhu, H.; Lee, B.; Amiridis, M. D.; Dai, S. *Catal. Lett.* **2004**, *95*, 99.
(25) Sanchez, A.; Abbet, S.; Heiz, U.; Schneider, W.-D.; Häkkinen, H.; Barnett, R. N.; Landman, U. *J. Phys. Chem. A* **1999**, *103*, 9573.
(26) Häkkinen, H.; Abbet, W.; Sanchez, A.; Heiz, U.; Landman, U. *Angew. Chem., Int. Ed.* **2003**, *42*, 1297.
(27) Lee, S.; Fan, C.; Wu, T.; Anderson, S. L. *J. Am. Chem. Soc.* **2004**, *126*, 5682.
(28) Herzing, A. A.; Kiely, C. J.; Carley, A. F.; Landon, P.; Hutchings, G. J. *Science* **2008**, *321*, 1331.
(29) Häkkinen, H. *Chem. Soc. Rev.* **2008**, *37*, 1847.
(30) Furche, F.; Ahlrichs, R.; Weis, P.; Jacob, C.; Gilb, S.; Bierweiler, T.; Kappes, M. M. *J. Chem. Phys.* **2002**, *117*, 6982.
(31) Häkkinen, H.; Yoon, B.; Landman, U.; Li, X.; Zhai, H.-J.; Wang, L.-S. *J. Phys. Chem. A* **2003**, *107*, 6168.

whereas at $n = 12$ there is a crossover where both 2D and 3D structures are present. For $n = 13$, ion mobility data[30] point to a 3D structure being more stable, whereas electron diffraction[32] and photoelectron[31] data rather indicate an isomeric mixture. Cationic gold clusters have been found to assume a 2D structure for $n \leq 7$, with a crossover to 3D structures for $n \geq 8$.[33]

The original ion mobility measurements were combined with DFT calculations that found 2D structures to be the more-stable configurations for Au_{13}^- and Au_8^+, in disagreement with the experimental findings.[30,33] Several studies have elaborated on these early works by considering more structures and other GGA functionals, but still it seems that DFT is not successful in predicting the correct structures.[29]

One virtue of GGA functionals is that they largely solve the overbinding problem of the local density approximation (LDA). This is achieved through the gradient enhancement factor, which increases the (negative) exchange contribution to the total energy in regions where the electron charge decays. Since atoms have more such regions than molecules, clusters, and crystals, the gradient enhancement shifts the energy balance in favor of atoms and thereby eliminates the overbinding problem. Likewise, when two isomers of a given atomic cluster size are compared, addition of gradient enhancement in the GGA form favors the more-open structure. The degree of gradient enhancement present in a GGA thus influences the relative stability of two such isomers, which explains why competing GGAs may produce opposite results for a given problem.

More importantly, since the gradient enhancement depends on only one property, the reduced density gradient, GGAs do not offer much flexibility in attempts to accurately reproduce several properties, such as the atomization energy and the relative stability of competing isomers. A natural step forward from the GGAs would be to consider meta-generalized gradient approximation (MGGA) functionals, which include the kinetic energy density in the functional expression.

In this work, we investigated the transition between 2D and 3D cluster shapes for anionic and cationic Au clusters using two MGGAs, the TPSS and the M06-L functionals, which are very different in their construction. The TPSS functional[34] was constructed by subjecting the form of the functional to a number of exact constraints, whereas the M06-L[35] was constructed by fitting a highly parametrized functional form (containing 25 parameters) to a large database of organic and organometallic compounds. The M06-L functional has recently proven to be successful in several applications.[36−38] Comparison of our M06-L results to PBE and TPSS values shows the good performance of M06-L for both cationic and anionic clusters. Previously, Johansson et al.[39] reported the first MGGA calculations on an anionic gold cluster, finding a preference for a 3D structure for $n = 13$ when using the TPSS[34] functional. We extend that study substantially by considering both cationic and anionic clusters. Furthermore, we point out in detail the factors that allow the MGGAs to give good results both for the relative stability of competing gold isomers and for the atomization energies.

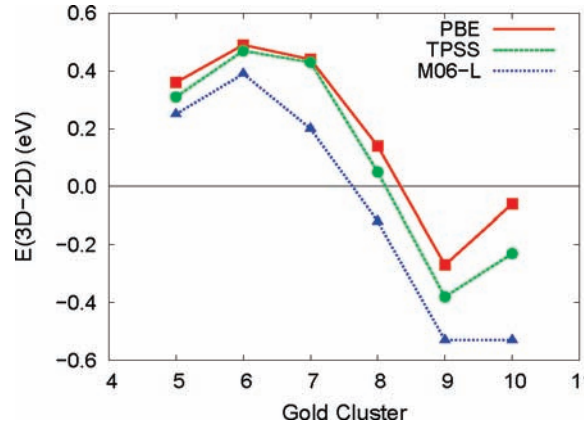

Figure 1. Energy difference between the lowest 3D and 2D structures for the cationic clusters investigated in this work at the PBE, TPSS, and M06-L levels of theory. The crossover between the 2D and 3D structures occurs at $n > 8$ for PBE and TPSS and $n > 7$ for M06-L.

Computational Details

The structures of the gold clusters employed in this work were taken from refs 30, 31, 33, and 39 and optimized with the PBE GGA functional.[40] The structures considered and energy orderings found are included in the Supporting Information.

The single-point energies at the PBE-optimized geometry and density were calculated using the PBE functional and the TPSS[34] and M06-L[35] MGGA functionals, as implemented in a local version of the Grid-Based Projector-Augmented Wave (GPAW) code.[41,42] An additional set of energies were obtained for some anionic clusters using the TPSS-optimized geometries from ref 39. These results are also reported in the Supporting Information.

The energies were converged to a threshold of 0.001 eV/atom using a grid spacing of 0.14 Å and a space of 6 Å between the cluster and the wall of the cell. A smaller grid size of 0.12 Å was tested for Au_8^+ and Au_8^- and gave only small changes in the final energy differences. No periodicity was applied. Spin polarization was not considered, but a test on Au_{12}^- confirmed that it was negligible.

All of the calculations presented were performed with the standard GPAW gold setups.[42] We tested the results for smaller sphere sizes but found only negligible changes. Furthermore, the optimal values of the lattice constant, a, for face-centered cubic Au (FCC-Au) obtained using PBE, TPSS, and M06-L were 4.17, 4.13, and 4.16 Å, respectively. The PBE and TPSS values are in good agreement with earlier results.[43] The M06-L value is the first published for FCC-Au.

Results and Discussion

Isomer Stability. In this section, we will first discuss the results obtained for the cationic clusters and then those for the anionic clusters.

The energy differences between the most stable 3D and 2D cationic structures for $n = 5-10$ are shown in Figure 1. In agreement with earlier studies, our PBE calculations indicate

(32) Xing, X.; Yoon, B.; Landman, U.; Parks, J. H. *Phys. Rev. B* **2006**, *74*, 165423.
(33) Gilb, S.; Weis, P.; Furche, F.; Ahlrichs, R.; Kappes, M. M. *J. Chem. Phys.* **2002**, *116*, 4094.
(34) Tao, J.; Perdew, J. P.; Staroverov, V. N.; Scuseria, G. E. *Phys. Rev. Lett.* **2003**, *91*, 146401.
(35) Zhao, Y.; Truhlar, D. G. *J. Chem. Phys.* **2006**, *125*, 194101.
(36) Zhao, Y.; Truhlar, D. G. *J. Am. Chem. Soc.* **2007**, *129*, 8440.
(37) Fedorov, A.; Moret, M.-E.; Chen, P. *J. Am. Chem. Soc.* **2008**, *130*, 8880.
(38) Benitez, D.; Tkatchouk, E.; Yoon, I.; Stoddart, J. F.; Goddard, W. A., III. *J. Am. Chem. Soc.* **2008**, *130*, 14928.
(39) Johansson, M. P.; Lechtken, A.; Schooss, D.; Kappes, M. M.; Furche, F. *Phys. Rev. A* **2008**, *77*, 053202.
(40) Perdew, J. P.; Burke, K.; Ernzerhof, M. *Phys. Rev. Lett.* **1996**, *77*, 3865.
(41) Blöchl, P. E. *Phys. Rev. B* **1994**, *50*, 17953.
(42) Mortensen, J. J.; Hansen, L. B.; Jacobsen, K. W. *Phys. Rev. B* **2005**, *71*, 35109.
(43) Haas, P.; Tran, F.; Blaha, P. *Phys. Rev. B* **2009**, *79*, 085104.

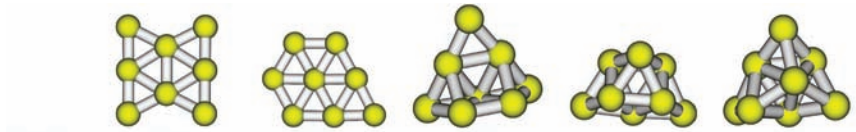

PBE	0.00	0.06	0.14	0.25	0.31
TPSS	0.00	0.04	0.05	0.10	0.15
M06-L	0.12	0.14	0.03	0.00	0.02

Figure 2. Structures for Au_8^+ from left to right: D_{2h}, C_{2v}, C_s, C_{2v}-II, and C_s-II. The table gives the calculated energy differences (in eV) with respect to the most stable structure at the PBE, TPSS, and M06-L levels of theory.

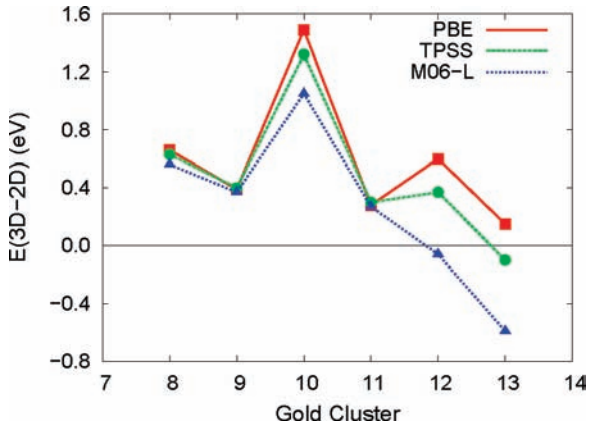

Figure 3. Energy difference between the lowest 3D and 2D structures for the anionic clusters investigated in this work at the PBE, TPSS, and M06-L levels of theory. The crossover between the 2D and 3D structures occurs at $n > 13$ for PBE and TPSS and $n > 12$ for M06-L.

that the 2D structures have the lower energy up to $n = 8$, a conclusion that is inconsistent with the ion mobility data.[33] The TPSS functional finds the 2D structure to be more stable by a small energy difference relative to the lowest 3D one when $n = 8$. The M06-L functional shows a markedly different behavior, giving a clear crossover to a 3D structure for $n \geq 8$, in agreement with experiment. This result is further illustrated in Figure 2, where the energies for the different Au_8^+ structures are reported. PBE finds the 2D structures to be close in energy and much lower than all of the 3D structures, while TPSS finds a 2D structure to be lowest in energy, just slightly lower than a 2D and a 3D structure that are almost degenerate. In contrast, M06-L shows the 2D structures to be higher in energy than all of the 3D structures, which are almost degenerate.

A similar good performance for the M06-L functional was identified in the calculation of the energies of negatively charged Au clusters. Experimentally, anionic gold clusters with $n \leq 11$ are found to be planar, whereas for Au_{12}^-, a mixture of 2D and 3D isomers is found; for $n > 12$, 3D structures are found to be more stable.[30] Our calculations using each of the functionals suggest that Au_n^- ($n \leq 11$) have planar ground states (Figure 3). PBE and TPSS indicate that Au_{12}^- has a planar ground state by a large energy difference; in contrast, M06-L predicts a 3D structure to be the lowest in energy by a small energy difference (0.06 eV), in good agreement with the isomeric mixture of 2D and 3D structures observed experimentally.[30] For Au_{13}^-, the ground state is again dependent on the functional: PBE predicts a planar structure, whereas both MGGA functionals predict a 3D structure. PBE finds the lowest 2D structures to be almost degenerate and far in energy from the 3D structures; TPSS finds the lowest 3D structures to be almost degenerate and ∼0.10 eV lower than the 2D structures, whereas M06-L predicts the 3D structures to be ∼0.60 eV lower than the 2D structures (see Figure 4).

Our PBE and TPSS results are in good agreement with earlier results.[39] Before accounting for various corrections (compare Tables III and IV of ref 39), Johansson et al. found the second 2D structure, 13-III in Figure 4 (the first structure, 13A, was not considered), to be 0.23 eV lower and 0.08 eV higher in energy than the last 3D structure, 13-I, using PBE and TPSS, respectively.[39] Our calculations give values of 0.17 and 0.06 eV, respectively, for the same energy differences, which is a fair agreement considering that different basis sets were used here and in ref 39.

Functional Form. In this section, we will try to understand the success of the MGGAs in predicting the correct crossover. One thing that is clear is that the kinetic energy favors the open 2D structures while the exchange energy (because of the $n^{4/3}$ scaling) favors the compression of the electrons in the more compact 3D structures. It has previously been recognized that the planar structures are energetically relevant only because of the proximity of the 5d and 6s levels of gold, which allows for a lowering of the kinetic energy.[44,45]

When discussing the influence of gradient and kinetic energy densities, we will focus on the exchange enhancement factor, F_x, defined as

$$E_x = \int F_x[n(\mathbf{r}),\ \nabla n(\mathbf{r}), \tau(\mathbf{r})]\ \varepsilon_x^{LDA}[n(\mathbf{r})]\ d^3\mathbf{r} \qquad (1)$$

where E_x is the exchange energy, $\varepsilon_x^{LDA}[n(\mathbf{r})]$ is the local exchange energy density at point $\mathbf{r}$, and $\tau(\mathbf{r})$ is the kinetic energy density at $\mathbf{r}$. We focus on the exchange, as it is a much larger effect than correlation for the present systems. To understand the effect of F_x, we will use the following two reduced dimensionless quantities:

$$s = \frac{|\nabla n|}{2(3\pi^2)^{1/3} n^{4/3}}, \quad \alpha = \frac{\tau - \tau^W}{\tau^{LDA}} \qquad (2)$$

where τ^W is the von Weizsäcker kinetic energy density.

Building an intuition about the reduced density gradient s is quite simple. Since $s \propto an^{-1/3}$, it diverges for an exponentially decreasing density $n(r) = b\exp(-ar)$. Large reduced gradients are thus mainly found in the density tails of atoms, molecules, and clusters, as illustrated for the gold dimer, Au_2, in Figure 5a.

Since F_x usually increases monotonically from unity at $s = 0$, it becomes clear that GGAs with a large gradient enhancement favor the open 2D structures while those with a smaller exchange enhancement than PBE favor 3D structures. Figure 6

(44) Häkkinen, H.; Moseler, M.; Landman, U. *Phys. Rev. Lett.* **2002**, *89*, 033401.
(45) Grönbeck, H.; Broqvist, P. *Phys. Rev. B* **2005**, *71*, 073408.

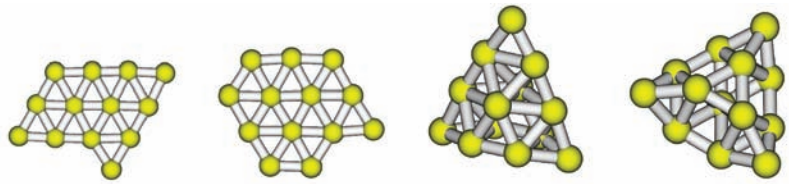

PBE	0.00	0.03	0.15	0.20
TPSS	0.11	0.10	0.00	0.04
M06-L	0.62	0.59	0.03	0.00
PBE$\frac{1}{2}$	0.10	0.07	0.00	0.03
PBEsol	0.27	0.19	0.00	0.02

Figure 4. Structures for Au_{13}^- from left to right: 13A, 13-III, 13C, and 13-I. The table gives the calculated energy differences (in eV) with respect to the most stable structure at the PBE, TPSS, M06-L, PBE(1)/(2), and PBEsol levels of theory.

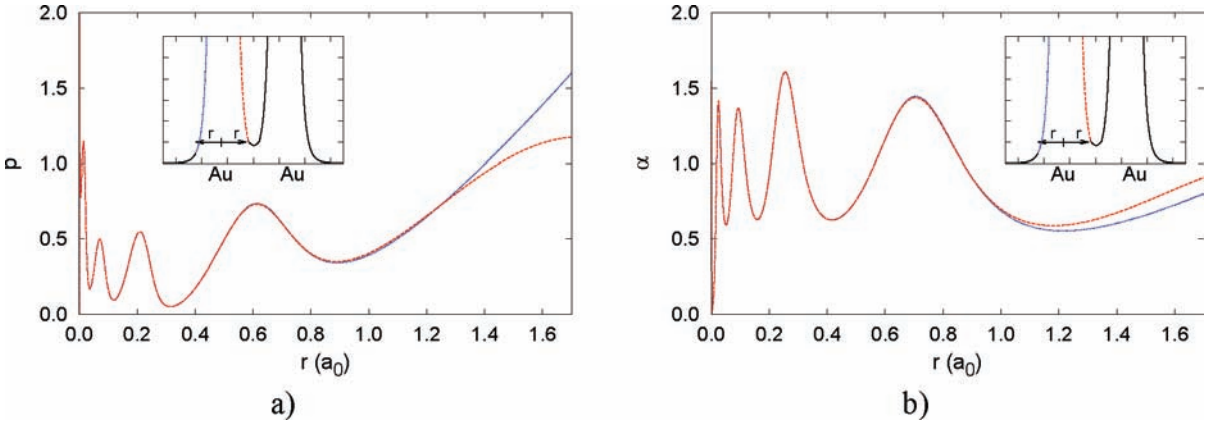

Figure 5. Reduced quantities (left) $p = s^2$ and (right) α for Au_2. The insets show the all-electron density, and the blue and red colors are used to label the tail and bonding regions, respectively. The reduced quantities are compared for these two regions as a function of the distance to the nuclear position.

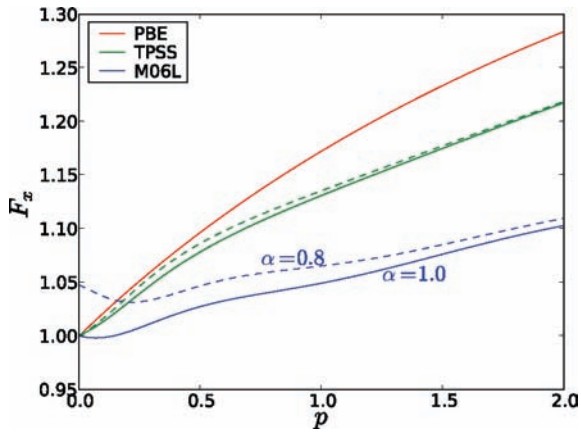

Figure 6. Exchange enhancements F_x as function of $p = s^2$ for various functionals. For the MGGA functionals, the solid lines are for $\alpha = 1.0$ and the dashed lines for $\alpha = 0.8$.

shows that both TPSS and M06-L have a smaller gradient enhancement than PBE, which immediately explains their stronger tendency to give 3D structures.

The above discussion shows that the increased tendency to give 3D structures that is needed for agreement with experiment could also have been achieved by using a GGA with a smaller gradient enhancement, such as the PBE(1)/(2)[46] or PBEsol functional.[47] In Figure 4, we report the PBE(1)/(2) and PBEsol values obtained at the PBE optimized geometry for the Au_{13}^- clusters, which show that for these two functionals, the 3D structures are indeed preferred to the 2D ones, as expected. This immediately explains why Johansson et al.[39] found that PBEsol favors the 3D structures for anionic gold. The performance of PBEsol was attributed to the jellium surface energy constraint, but we challenge this interpretation, as the result could equally well have been achieved with another GGA with a smaller exchange enhancement.

Table 1. Bond Energies for Gold Dimer, Au_2, from Experiment and Calculated with Five Different Functionals

	exptl[a]	PBE	PBE½	PBEsol	TPSS	M06-L
E_b (eV)	−2.30	−2.27	−2.43	−2.52	−2.27	−2.35

[a] From ref 49.

The problem with using GGAs with a smaller gradient enhancement is that such functionals in turn tend to overestimate the bonding energy (like the LDA). As an example, we considered the bond energy of the gold dimer, Au_2. Our results are shown in Table 1. The GGAs with smaller exchange enhancement, PBE(1)/(2) and PBEsol, provide poor results for the dimer bond energy, while the MGGAs give excellent agreement with experiment. The interesting question is thus how the MGGAs manage to increase the 3D tendency *and* give a good prediction of the bond energy.

The answer to this obviously lies in the additional functional dependence of the MGGAs on the kinetic energy term, which we will analyze in terms of α. To build an intuition about α, we note that it is the main ingredient in the widely used electron

(46) Madsen, G. K. H. *Phys. Rev. B* **2007**, *75*, 195108.
(47) Perdew, J. P.; Ruzsinszky, A.; Csonka, G. I.; Vydrov, O. A.; Scuseria, G. E.; Constantin, L. A.; Zhou, X.; Burke, K. *Phys. Rev. Lett.* **2008**, *100*, 136406.
(48) Becke, A. D.; Edgecombe, K. E. *J. Chem. Phys.* **1990**, *92*, 5397.

localization function[48] and is related to the curvature of the exchange hole. Furthermore, $\tau = \tau^W$ for an iso-orbital region. In Figure 5b, we plot α as a function of the distance from one Au core in the gold dimer. As in Figure 5a, the red curve is for the direction of the chemical bond, while the blue curve is for the opposite direction, toward the apex of the dimer. In the bonding region, α is significantly higher than in the nonbonding region. This is expected since the nonbonding region becomes increasingly dominated by one orbital (the Au 6s) as the distance from the nuclear position increases. The MGGA functionals use the information from both *s* and α and can treat the exchange enhancement differently in regions with chemical bonding and regions with decaying density tails. With the energy ordering of the isomers improved by the decreased dependence on *s*, as discussed above, MGGAs have the possibility to adjust the bonding energies independently. As illustrated in Figure 6 for two values of α, the MGGAs reduce the exchange enhancement with increasing α, which counteracts the increased bonding energy obtained by reducing the gradient enhancement.

Conclusion

We have presented a DFT study of both cationic and anionic gold clusters that shows the good performance of the MGGA functionals with respect to GGA functionals. The overall performance of M06-L is quite remarkable, since it places the 2D−3D transition for cationic clusters at $n > 7$ and that for anionic clusters at $n > 11$, as suggested by experiments. We have stressed that the reason for the good performance of MGGAs, both for bond energies and the relative stability of competing gold clusters, arises from their ability to use the information contained in both the reduced gradient and the kinetic energy, which is strictly necessary in our study.

Acknowledgment. This work was supported by the Danish Research Councils and the Danish Center for Scientific Computing.

Note Added in Proof. After acceptance of our paper we have learned that M. Mantina, R. Valero and D. G. Truhlar have submitted a comparable study of the shape of anionic Au clusters in which they reach similar conclusions.

Supporting Information Available: Structures of the gold clusters considered and their energy ordering for the different fuctionals employed in this work. This material is available free of charge via the Internet at http://pubs.acs.org.

JA903069X

(49) Morse, M. D. *Chem. Rev.* **1986**, *86*, 1049.